

2016

# A histological analysis of the role of a LOX-PP variant in breast cancer, leukemia, and lymphoproliferative disease

---

<https://hdl.handle.net/2144/16746>

*"Downloaded from OpenBU. Boston University's institutional repository."*

BOSTON UNIVERSITY  
SCHOOL OF MEDICINE

Thesis

**A HISTOLOGICAL ANALYSIS OF THE ROLE  
OF A LOX-PP VARIANT IN BREAST CANCER, LEUKEMIA,  
AND LYMPHOPROLIFERATIVE DISEASE**

by

**MICHAEL EMMERLING**

B.S., Boston College, 2014

Submitted in partial fulfillment of the  
requirements for the degree of  
Master of Science

2016

© 2016 by  
MICHAEL EMMERLING  
All rights reserved

Approved by

First Reader

---

Kathrin H. Kirsch, Ph.D.  
Associate Professor of Biochemistry

Second Reader

---

Karen Symes, Ph.D.  
Associate Professor of Biochemistry

## **ACKNOWLEDGMENTS**

I would like to thank Dr. Kathrin Kirsch, Dr. Ana de la Cueva, and Dr. Matthew Layne for their guidance in the laboratory and for their assistance in making this thesis. I would also like to thank Dr. Karen Symes and Dr. Gwynneth Offner for their encouragement and advice over the course of the past two years. I would like to extend my appreciation to my roommates Bradley Pearson, Michael Park, William Stevens, and Hussein Abdurassoul for their support and also to Carl Ceraolo, my colleague in the lab.

# A HISTOLOGICAL ANALYSIS OF THE ROLE OF A LOX-PP VARIANT IN BREAST CANCER, LEUKEMIA, AND LYMPHOPROLIFERATIVE DISEASE

MICHAEL EMMERLING

## ABSTRACT

**Background:** In their lifetime, 42% of men and 38% of women will be diagnosed with cancer. One of the most prominent cancers in women is breast cancer, which represents 14.8% of newly diagnosed cancers. Research has demonstrated the importance of the lysyl oxidase (*LOX*) gene, more specifically the lysyl oxidase propeptide (*LOX-PP*), in the attenuation of breast cancer and in mouse xenograft models, making it an important and ongoing area of investigation. In recent, unpublished experiments, mice with a variant of *LOX-PP* were treated with 7,12-Dimethylbenz[*a*]anthracene (*DMBA*) to induce breast cancer. However, some of the treated mice developed poor body conditions without any signs of having developed breast cancer. Published studies have demonstrated that, following treatment with *DMBA*, some mice generate leukemia or other lymphoproliferative diseases. Research has shown that identification of these diseases is possible via histological analyses or immunohistochemistry.

**Objective:** To determine the cause of poor body conditions in mice treated with *DMBA* that did not develop mammary tumors by histological analyses and immunohistochemistry. Additionally, to determine the difference between a

variant of LOX-PP (LOX-PP<sub>v</sub>) knock-in (K<sub>i</sub>) and wild type (WT) mice in the generation of poor body conditions or leukemia/lymphoproliferative disease.

**Methods:** A total of 48 mice, 24 LOX-PP<sub>v</sub> K<sub>i</sub> and 24 WT, were treated with DMBA and observed for mammary tumor formation. Body conditions of the mice were observed and noted, and liver samples from these mice were obtained and analyzed via histological and immunohistochemistry interventions. In Hematoxylin & Eosin (H&E) assessments of mice livers, mice were classified as normal or as having possible lymphocyte infiltration, mild lymphocyte infiltration, or massive lymphocyte infiltration. Staining with the Ki-67 antibody in immunohistochemistry allowed for classification of mouse livers as normal or as having slightly positive or massively positive expression of the Ki-67 antigen. The degree to which each liver sample was positive for both readings was compared and further analyzed.

**Results:** A total of 9 mice (30.4% of K<sub>i</sub> mice and 8.7% of WT mice) displayed poor body conditions following DMBA treatment. Of the 9 (7 K<sub>i</sub> and 2 WT) mice having poor body condition, 2 K<sub>i</sub> mice suffered from severe dermatitis. For the 7 remaining mice, no cause for such poor body conditions was obvious. 6 of these mice (85.7%) were diagnosed with leukemia. In all other DMBA-treated mice, 52.6% of K<sub>i</sub> and 23.8% of WT displayed some degree of abnormal lymphocyte infiltration in the liver, while a total of 39.1% of the K<sub>i</sub> mice and 69.6% of the WT mice had normal liver histologies. 60.9% of K<sub>i</sub> and 45.5% of WT mice displayed some degree of positivity for expression of Ki-67.

**Conclusions:** Mice not diagnosed with breast cancer but that were suffering from poor body conditions likely had developed leukemia or some other lymphoproliferative disease. In the mice not definitively diagnosed with leukemia by a pathologist, H&E analyses and immunohistochemistry of the livers showed lymphocyte infiltration and cellular proliferation possibly indicative of leukemia., but further tests are necessary to confirm this. Furthermore, LOX-PP<sub>v</sub> K<sub>i</sub> mice appeared to have a greater likelihood of generating poor body conditions or some observable sign of abnormal lymphocyte infiltration in the liver versus their WT counterparts when treated with DMBA.

## TABLE OF CONTENTS

|  |      |
|--|------|
| TITLE.....                                   | i    |
| COPYRIGHT PAGE.....                          | ii   |
| READER APPROVAL PAGE.....                    | iii  |
| ACKNOWLEDGMENTS.....                         | iv   |
| ABSTRACT .....                               | v    |
| TABLE OF CONTENTS .....                      | viii |
| LIST OF TABLES .....                         | x    |
| LIST OF FIGURES .....                        | xi   |
| LIST OF ABBREVIATIONS .....                  | xii  |
| INTRODUCTION.....                            | 1    |
| Cancer: by the Numbers .....                 | 1    |
| Causes and characteristics of cancer .....   | 1    |
| Breast cancer: an overview .....             | 3    |
| Lysyl oxidase: role in cancer .....          | 5    |
| LOX-PP Variant: Arg158Gln substitution ..... | 8    |
| Leukemia, DMBA, and the Liver .....          | 9    |
| HYPOTHESES AND GOALS.....                    | 11   |
| MATERIALS AND METHODS.....                   | 12   |

|                       |    |
|-----------------------|----|
| RESULTS .....         | 25 |
| DISCUSSION.....       | 37 |
| REFERENCES .....      | 41 |
| CURRICULUM VITAE..... | 46 |

## LIST OF TABLES

| Table | Title  | Page |
|-------|--|------|
| 1     | Results of Hematoxylin and Eosin Staining of K <sub>i</sub> Mouse Livers | 28   |
| 2     | Results of Hematoxylin and Eosin Staining of WT Mouse Livers             | 29   |
| 3     | Results of Ki-67 Antibody Immunohistochemistry of K <sub>i</sub> Mice    | 32   |
| 4     | Results of Ki-67 Antibody Immunohistochemistry of WT Mice                | 33   |

## LIST OF FIGURES

| Figure | Title  | Page |
|--------|--|------|
| 1      | Livers stained with Hematoxylin and Eosin  | 27   |
| 2      | Lymphocyte infiltration in livers in LOX-PP K <sub>i</sub> vs. WT mice after treatment with DMBA | 30   |
| 3      | Livers stained with Ki-67 antibody   | 35   |
| 4      | Expression of Ki-67 in LOX-PP K <sub>i</sub> vs. WT mice after treatment with DMBA               | 36   |

## LIST OF ABBREVIATIONS

|                                     |                                      |
|-------------------------------------|--------------------------------------|
| ACS.....                            | American Cancer Society              |
| AhR.....                            | Aryl hydrocarbon receptor            |
| BMP1.....                           | Bone morphogenetic protein 1         |
| cDNA.....                           | complementary DNA                    |
| DMBA.....                           | 7,12-Dimethylbenz[a]anthracene       |
| ECM.....                            | Extracellular matrix                 |
| EMT.....                            | Epithelial to mesenchymal transition |
| ER.....                             | Estrogen receptor                    |
| EtOH.....                           | Ethanol                              |
| H <sub>2</sub> O <sub>2</sub> ..... | hydrogen peroxide                    |
| H&E.....                            | Hematoxylin & Eosin stain            |
| HCl.....                            | Hydrochloric acid                    |
| kDa.....                            | Kilodaltons                          |
| K <sub>i</sub> .....                | Knock-in                             |
| LOX.....                            | Lysyl oxidase                        |
| LOX-PP.....                         | Lysyl oxidase propeptide             |
| LOX-PP <sub>v</sub> .....           | variant lysyl oxidase propeptide     |
| NF-κB.....                          | Nuclear factor-κB                    |
| NRKF.....                           | Normal rat kidney fibroblasts        |
| PAH.....                            | Polycyclic aromatic hydrocarbon      |
| PBS.....                            | Phosphate buffered saline            |

Pro-LOX.....Lysyl oxidase proenzyme  
RFLP.....restriction fragment length polymorphism  
*rrg*.....Ras recision gene  
RT.....Room temperature  
SNP.....Single nucleotide polymorphism  
UV.....Ultraviolet  
WT.....Wild type

## INTRODUCTION

### ***Cancer: by the Numbers***

Cancer is a collection of diseases characterized by aberrant growth and dissemination of abnormal cells and is the second most common cause of death in the US, behind only heart disease. In total, the American Cancer Society (ACS) estimates that approximately 1,658,210 individuals will be diagnosed with cancer in 2016, while over the course of a lifetime men in the US have a 42% chance and women have a 38% chance of developing cancer. Despite significant advancements in cancer detection and treatment, the mortality rate for cancer reaches approximately 30% (American Cancer Society, 2016). It is thus important for researchers to investigate the mechanisms behind the generation and propagation of cancer so that treatments can be formulated to specifically target and combat cancer before it progresses to the point of fatality.

### ***Causes and characteristics of cancer***

While some cancers are the result of external factors like tobacco or infectious organisms, others can be the result of genetic mutations or other health conditions and infectious agents (American Cancer Society, 2016); the bacteria *Helicobacter pylori*, for example, has been implicated in the generation of stomach cancer (American Cancer Society, 2016; Hwang et al., 2015). These inherited or acquired genetic predispositions can act in combination with external

stimuli to result in or increase the likelihood of cancer by allowing for the acquisition and subsequent propagation of cancerous traits (American Cancer Society, 2016; Hanahan & Weinberg, 2011).

Debatably the most essential trait of the six “hallmark features” of cancerous cells is their ability to proliferate uncontrollably via deregulation of normal cell proliferative signals. Normal cells exhibit a controlled and carefully regulated cell growth cycle, which promotes and maintains homeostatic conditions that are favorable to the essential functioning of tissues and organs (Hanahan & Weinberg, 2011). Cancerous cells, on the other hand, hijack and thereafter deregulate these signaling pathways in order to proliferate indefinitely and disrupt normal biological processes (American Cancer Society, 2016; Hanahan & Weinberg, 2011). In addition to uncontrolled cell growth and proliferation is the ability of cancerous cells to evade growth suppressors and resist cell death. This is often the result of the inactivation of tumor suppressor genes, often via somatic or germ-line mutations, which allows cancerous cells to avoid senescence or apoptotic signaling and continue to proliferate. Under normal cellular conditions, this apoptotic signaling prevents further propagation of cells that are structurally compromised or that contain significant damage to DNA that might have been acquired via genetic mutations or other external factors such as carcinogens or ultraviolet (UV) light (Hanahan & Weinberg, 2011).

Another hallmark of cancerous cells is the ability of these cells to sustain themselves with necessary nutrients and oxygen via angiogenesis. Furthermore,

these cells are able propagate and spread via the activation of metastatic signaling and pathways that increase cellular invasiveness. Studies have shown that these metastatic cancer cells typically develop morphological changes and display altered associations with surrounding cells and the extracellular matrix (ECM). Especially observable in aggressive carcinomas, cancerous cells often exhibit compromised cell-to-ECM interactions and an up-regulation of adhesion molecules typically associated with cellular migration seen in embryogenesis and inflammation (Hanahan & Weinberg, 2011). Together, these acquired traits permit normal cells within the body to become tumorigenic and are ultimately detrimental to the health of the host organism (Hanahan & Weinberg, 2011).

### ***Breast cancer: an overview***

Breast cancer is a subset of cancer that represents approximately 14.8% of newly diagnosed cancers (American Cancer Society, 2016). As such, breast cancers is established as one of the most common cancers in women and represents the second most common cause of premature female mortality in Western countries (Oeffinger, Fontham, Etzioni, et al., 2015; Zhang et al., 2015). Despite its prevalence, recent technological and scientific advances in the detection and treatment of breast cancer have resulted in a steady decline of mortality rates since 1990 (Oeffinger, Fontham, Etzioni, et al., 2015). There still remains, however, a high likelihood of mortality from failed therapeutic treatments, which are often the result of metastasis and invasiveness of the

cancerous cells (Liu et al., 2012). Studies have found that, of those patients diagnosed with breast cancer, 10-15% will develop metastases within three years (Chan et al., 2015). Beyond this three-year mark, anywhere from 25-50% of patients diagnosed with breast cancer develop metastases, even when the primary tumor has been successfully eradicated or removed (Lorusso & Rüegg, 2012). Formation and progression of these tumor metastases is negatively correlated with patient prognosis and survival (Zhang et al., 2015).

The liver is among one of the more prominent sites of metastasis in many cancers, including breast cancer, and is the primary organ of interest in our study (Tabariès et al., 2015); other common sites of breast cancer metastases include the lung, brain, and bone (Lorusso & Rüegg, 2012). As the liver is responsible for a number of vital functions like detoxification and metabolism of nutrients, infiltration of metastatic cancerous cells poses a serious threat to the health and well-being of affected patients (Lorusso & Rüegg, 2012; McCuskey, 2012). The liver is also frequently involved in lymphoproliferative diseases such as lymphomas and leukemia (Baumhoer et al., 2008). Though primary hepatic lymphomas are rare, the liver is often a secondary site of infiltration for neoplastic cells that arise from lymphoproliferative diseases such as B- and T-cell lymphomas and Hodgkin's lymphoma (Baumhoer et al., 2008). It is therefore of paramount importance to investigate and identify the mechanisms by which breast cancer or other lymphoproliferative diseases metastasize to or manifest within the liver or to other organs throughout the body. These advancements

could drastically improve patient prognosis by allowing for a more effective and focused treatment of the cancer.

### ***Lysyl oxidase: role in cancer***

Lysyl oxidase (LOX) is an important protein in tumor suppression and metastasis. It is a copper-dependent amine oxidase that functions to crosslink collagens and elastins within the extracellular matrix (ECM), stabilizing collagen fibrils and promoting elasticity of elastin in order to preserve tissue integrity (Csiszar, 2001; Liu et al., 2012; Nishioka, Eustace, & West, 2012). The *LOX* gene, which encodes the LOX protein, has been isolated and shown to encode a 50kDa lysyl oxidase proenzyme (Pro-LOX) which is proteolytically cleaved by bone morphogenetic protein 1 (BMP1) in the extracellular environment to yield the 32kDa LOX enzyme and an 18 kDa propeptide (LOX-PP) (Min et al., 2010; Nishioka, Eustace, & West, 2012; Barker, Cox, & Eler, 2012). The enzyme portion of LOX is encoded for by the C-terminal end of the *LOX* gene while the variable propeptide region resides within the N-terminal domain (Nishioka, Eustace, & West, 2012).

Studies have demonstrated that this 32kDa C-terminal product, the LOX enzyme, is responsible for the stabilization of the ECM (Nishioka, Eustace, & West, 2012). Interestingly, aberrant or uncontrolled expression of this LOX enzyme has been shown to be localized to pre-metastatic regions in orthotopic mouse models, suggesting that this LOX enzyme is conducive to or promotes

invasive and metastatic phenotypes (Nishioka, Eustace, & West, 2012; Barker, Cox, & Ertler, 2012). It is believed that this pathological phenotype arises as a result of increased ECM deposition and remodeling, which ultimately creates a microenvironment that supports homing of disseminated tumor cells.

Furthermore, this excessive remodeling of the ECM increases growth factor signaling that facilitates the formation and progression of tumors in the surrounding tissue (Barker, Cox, & Ertler, 2012). As our understanding of cancer as a highly complex organ has developed, this “tumor microenvironment” has been elucidated as an area of supreme importance in the understanding of tumorigenesis. This tumor microenvironment, as it has been coined by Hanahan, is composed of a number of supportive cells in the stroma surrounding the tumor. This dynamic support system is composed of cancer associated fibroblasts, endothelial cells, pericytes, and immune inflammatory cells that are constantly evolving and adapting to support and maintain the tumor (Hanahan & Weinberg, 2011).

The *LOX* gene has also been found to have tumor suppressor function (Barker, Cox, & Ertler, 2012). Originally referred to as the ras recision gene (*rrg*) (Contente, Kenyon, Rimoldi, & Friedman, 1990), *LOX* gene expression was found to oppose tumor progression through suppression of H-RAS-induced transformation of mouse fibroblasts (Barker, Cox, & Ertler, 2012). Subsequent studies further strengthened the idea that *LOX* had tumor suppressing properties via transfection of antisense *LOX* gene complementary DNA (cDNA) into normal

rat kidney fibroblasts (NRKFs). This ultimately resulted in an increase in the formation of tumors in nude mice (Barker, Cox, & Eler, 2012; Giampuzzi et al., 2001). Despite the general knowledge that the *LOX* gene had tumor suppressor function, the mechanisms by which this was accomplished were not elucidated for many years.

Recent studies have since attributed this tumor suppressor activity of the *LOX* gene to the highly conserved, N-terminal propeptide domain, the 18 kDa LOX-PP (Min et al., 2010; Barker, Cox, & Eler, 2012; Palamakumbura et al., 2004). Palamakumbura et al., for example, demonstrated that transfection of *ras*-transformed cells with LOX-PP inhibited the activation of nuclear factor- $\kappa$ B (NF- $\kappa$ B), which has been implicated in neoplastic transformation and aberrant cell growth (Min et al., 2007; Barker, Cox, & Eler, 2012; Palamakumbura et al., 2004; Jeay, Pianetti, Kagan, & Sonenshein, 2003). Further *in vitro* investigations demonstrated that this inhibition of NF- $\kappa$ B activation was via inhibition of the *ras*-dependent PI3K/PDK1/Akt signal transduction pathway (Palamakumbura et al., 2004). *In vivo* studies later corroborated these findings and further demonstrated the ability of LOX-PP to revert the invasive phenotype of Her-2/neu-driven cancer cells in mouse xenograft models (Min et al., 2007). Correspondingly, LOX-PP was found to reduce signaling via PI3K/Akt and MAPK/Erk pathways, as well as to reduce downstream NF- $\kappa$ B activity (Min et al., 2007). LOX-PP is the primary region of interest for our experiments on the generation and propagation of breast cancer and other lymphoproliferative diseases in mice.

### ***LOX-PP Variant: Arg158Gln substitution***

Follow-up studies on the protective effects of LOX-PP have found that a single nucleotide polymorphism (SNP, rs1800449), which causes a restriction fragment length polymorphism (RFLP) (Csiszar et al., 1993), in the N-terminal LOX-PP domain impairs the proteins tumor suppressor activity (Min et al., 2009). In humans, this SNP results in an Arg158Gln substitution within a highly conserved region of LOX-PP domain and prevents inhibition of the RAS signaling pathway, promoting the formation of xenograft tumors in mice (Min et al., 2009). Mice are the ideal candidates with which to study certain diseases affecting humans, as our genomes are 95% similar (Jong & Maina, 2010). In order to further study the effects of this SNP in vivo, a knock-in (K<sub>i</sub>) mouse line was developed wherein progeny carry an Arg152Gln substitution, corresponding to the Arg158Gln substitution found in humans. This mouse expresses a variant LOX-PP (LOX-PP<sub>v</sub>) compared to wild type (WT) mice that express LOX-PP (Cueva & Kirsch, unpublished)<sup>1</sup>.

To clarify the function of LOX-PP<sub>v</sub> in the formation of breast and other cancers, WT and K<sub>i</sub> mice were treated with medroxyprogesterone and 7,12-Dimethylbenz[a]anthracene (DMBA), a polycyclic aromatic hydrocarbon (PAH) and tumor formation was observed. DMBA has been demonstrated to lead to

---

<sup>1</sup> Unpublished study conducted by Dr. Ana de la Cueva and Dr. Kathrin H. Kirsch in the Biochemistry Department at the Boston University School of Medicine.

mammary gland tumors in mice. Tumors in these mice displayed up-regulation of oncogenic signaling pathways including elements of the Wnt signaling pathway, the prolyl isomerase Pin-1, and the NF- $\kappa$ B pathway (Currier et al., 2005).

### ***Leukemia, DMBA, and the Liver***

DMBA has also been demonstrated to induce, to a lesser degree, leukemia in rodents. As the leukemia develops, leukemic cells have been detected primarily within the liver and spleen (Huggins & Sugiyama, 1966). These mice also displayed a decrease in body weight and experience splenomegaly, often developing to the point where the liver is palpable from the outside (Huggins & Sugiyama, 1966).

Hepatic biopsy and subsequent histological analysis is one technique for detecting leukemia. Histological and immunohistochemical examination of these organs allows for the visualization of the invasion of large blast cells in the hepatic sinusoids and in the red pulp or lymph follicles of the spleen. Leukemia-positive results present with dense clusters of basophilic cells in the sinusoids or portal triangles of the liver (Huggins & Sugiyama, 1966). Additionally, the expression of Ki-67, a nuclear protein associated with cellular proliferation, has been identified as an important diagnostic and prognostic tool in many types of neoplasms (Niikura et al., 2014; Scholzen & Gerdes, 2000). It is indicative of a poor prognosis in patients with estrogen receptor (ER)-positive breast cancer (Niikura et al., 2014; Scholzen & Gerdes, 2000). These findings allow for the

investigation and analysis of the effect of LOX-PP<sub>v</sub> on leukemia and lymphoproliferative disease formation in WT and K<sub>i</sub> mice via histological analysis and immunohistochemistry.

## HYPOTHESES AND GOALS

A Kaplan-Meier curve indicated that  $K_i$  mice treated with DMBA develop tumors earlier (50% of mice:  $K_i$ =16.5 weeks; WT=19 weeks) and are more likely to suffer from poor body condition in comparison to their WT counterparts (Cueva & Kirsch, unpublished)<sup>2</sup>. The majority of these mice ( $K_i$ =79.2%; WT=91.6%) developed breast cancer, but several other mice developed poor body conditions such as severe dermatitis, lung infections, or hepatomegaly without any explanation. As DMBA has been found to induce leukemia in mice (Huggins & Sugiyama, 1966), we hypothesized that the mice developing poor body conditions without explanation would show development of leukemia or lymphoma. Furthermore, given the protective function of LOX-PP, we hypothesized that leukemia and lymphoma development, if present, would be enhanced in  $K_i$  mice expressing LOX-PP<sub>v</sub> compared to WT mice expressing functional LOX-PP.

---

<sup>2</sup> Unpublished study conducted by Dr. Ana de la Cueva and Dr. Kathrin H. Kirsch in the Biochemistry Department at the Boston University School of Medicine.

## MATERIALS AND METHODS

### 1. Materials and Reagents

#### 1.1 Microscope Slide Coating

|   |   |
|---|---|
| <b>Chromium Potassium Sulfate Dodecahydrate</b> | Alfa Aesar (36715)                                |
| <b>Gelatin</b>                                  | Sigma Aldrich (G-6650)                            |
| <b>Microscope slides</b>                        | American Central Scientific Co. (FFP-001-010-F-1) |

#### 1.2 Hematoxylin and Eosin Staining

|  |                              |
|--|------------------------------|
| <b>1N Hydrochloric Acid</b>                  | American Bio (AB00831-01000) |
| <b>Ammonium Hydroxide</b>                    | American Bio (AB02333-02500) |
| <b>Eosin</b>                                 | Sigma Aldrich (HT110132-1L)  |
| <b>Graded ethanols (70%, 80%, 95%, 100%)</b> |                              |
| <b>Hematoxylin</b>                           | Sigma Aldrich (GHS332-1L)    |
| <b>Xylenes</b>                               | Fisher (UN1307)              |

#### 1.3 Immunohistochemistry Protocol

|  |                               |
|--|-------------------------------|
| <b>30% H<sub>2</sub>O<sub>2</sub></b>          | Fisher (H325-100)             |
| <b>Brij-35 powder</b>                          | Sigma Aldrich (P1254)         |
| <b>DAB Substrate Kit</b>                       | Vector Laboratories (SK-4100) |
| <b>Liquid Blocker Super Pap Pen</b>            | Daido Sangyo                  |
| <b>Normal Goat Serum Blocking Solution</b>     | Vector Laboratories (S-1000)  |
| <b>Phosphate Buffered Saline, 10X Solution</b> | Fisher (BP399-500)            |

|                                       |                               |
|---------------------------------------|-------------------------------|
| <b>Tri-sodium citrate (dehydrate)</b> | American Bio (AB01918-05000)  |
| <b>Tween 20</b>                       | American Bio (AB02038-00500)  |
| <b>Vectastain ABC Kit</b>             | Vector Laboratories (PK-6100) |

## **2. Antibodies**

|                                     |                               |
|-------------------------------------|-------------------------------|
| <b>Biotinylated anti-rabbit IgG</b> | Vector Laboratories (BA-1000) |
| <b>Ki-67 antibody</b>               | Thermoscientific (9106-S0)    |

## **3. Buffers and Solutions**

**Ammonia water.** Add 1.57 ml ammonium hydroxide to 500 ml dH<sub>2</sub>O.

**Acidified ethanol.** Add 5 ml concentrated HCl to 500 ml 70% EtOH.

**Cadenza Buffer.** This is essentially a Tris-buffered saline with Brij, a non-ionic detergent, instead of Triton. First, make standard Tris buffer (0.1 M, pH 7.6).

Then, add 1.0 g of Brij-35 powder per 1.0 L of 1X buffer.

**Sodium Citrate Buffer.** (10 mM sodium citrate, 0.05% Tween 20, pH 6.0)

Mix 2.94 g tri-sodium citrate (dehydrate) in distilled water until dissolved and bring the total volume to 1000 mL. Adjust pH to 6.0 with 1N HCl. Add 0.5 mL of Tween 20 and mix well. This solution can be stored at room temperature for 3 months or at 4°C for extended length.

## **4. Methods**

**4.1. Coating Microscope Slides with Gelatin.** This gelatin slide coating protocol coats microscope slides with a positive charge, allowing for stronger adhesion of negatively charged tissue sections. The following protocol is a modified version of an R&D Systems protocol (Protocol for the Preparation of Gelatin-coated Slides for Histological Tissue Sections, n.d.).

Prepare the gelatin-coating solution by heating 1.0 L of deionized H<sub>2</sub>O to approximately 40°C (do not exceed 45°C) and dissolving 5.0 g of gelatin into it. When the gelatin dissolves, add 0.5 g of chromium potassium sulfate dodecahydrate. This reagent will positively charge the slides, thereby attracting negatively charged tissue. The solution is then filtered using filter paper and a funnel. This solution can be stored at 2-8°C until use, at which time it is recommended that the solution be filtered once more before coating the slides. Adjust to room temperature before filtering a second time.

To begin coating the slides, place the microscope slides into glass slide holders. Dip the glass slide holders containing the histological slides into the gelatin-coating solution 3 to 5 times for approximately 5 seconds each time. Remove the slide holders containing the slides and then blot excess solution onto filter paper. The used gelatin solution can be saved and stored at 2-8°C for reuse.

Place slide holders containing the slides on filter paper and cover with paper towels. Let dry at room temperature for 48 hours. Dried slides can be put into boxes and stored at room temperature until use.

**4.2. Cutting Paraffin Sections.** Tissue samples were harvested from mice and embedded in paraffin. Sectioning the samples and mounting them on microscope slides allows for staining and visualization of desired tissue with a light microscope.

First obtain paraffin-embedded samples. To ensure clean cuts of the samples, place blocks of paraffin-embedded samples facedown on an ice tray that is covered with a wet paper towel. Let the samples sit on the ice tray for approximately 5 minutes before cutting.

Prior to cutting, cut the sample with a straight razor into a pyramid shape. Attempt to align edges and leave them parallel to one another. At this time, also prepare a water bath at 46-48°C for floating sections. 1.0 L of tap water can be heated in microwave for 2 minutes and poured into water bath to expedite the process. Repeat as necessary to obtain desired level of water.

Mount sample in the chuck of microtome, locking firmly into place. Then, mount blade in blade holder. Clean the blade with Q-tip soaked in Xylenes-substitute and ensure blade is dry before beginning to cut. Set the blade angle to 5°. Switch the lever on the right side of the microtome to unlocked position, allowing for movement of the chuck. Using the dial on the front of the microtome,

set the desired section thickness. For this experiment, liver sections were all cut at 5 $\mu$ m thickness.

Using the handle on the left side of microtome, align the sample block with the blade. Trim the block, if necessary, so that each cut produces uniform sections of the sample. To ensure a clean and uniformly exposed section, first trim sections at 20 $\mu$ m thickness until even sections of the sample are being cut each time. Be sure to reset the thickness to 5 $\mu$ m when obtaining samples.

Start sectioning. Use toothpicks to guide the unrolling of the sections. Place sections in water bath, carefully separating from toothpick to ensure the sample is not torn. Using gelatin coated slides (**Method 4.1**), sweep up samples from water bath. Label slides with sample type and number, sample thickness, and date.

Potential issues that can arise during cutting:

a. Sample is too curly: block is too cold. Warm with hot breath to smooth out the sections.

a. Sample is rigid or tearing easily: block is too hot. Cover an icepack with a damp paper towel and apply to block for 1:00 min.

i. Alternatively, the blade can be too dirty or dull. Clean or replace blade, or move the blade.

**4.3. H&E Staining.** This H&E Staining method is based on Bonna Ith's H&E Protocol, which was further revised by Dr. Matt Layne<sup>3</sup>. H&E staining allows for the visualization and discrimination of cell nuclei/chromatin, cytoplasm, collagen, and smooth muscle. It also allows for the visualization of basophilic cells such as lymphocytes that have infiltrated tissues and organs.

To begin, deparaffinize the samples by placing the slides for 10-15 minutes at 55-60°C in hybe oven or equivalent. Do not exceed 60°C. Samples are deparaffinized when the wax is melted and transparent. Rehydrate slides by dipping, sequentially, in the following reagents for the specified amount of time: Xylenes (5 minutes), Xylenes (5 minutes), 100% EtOH (2 minutes), 100% EtOH (2 minutes), 95% EtOH (2 minutes), 95% EtOH (2 minutes), 80% EtOH (2 minutes), dH<sub>2</sub>O (2 minutes).

Begin staining the slides by dipping, sequentially, in the following reagents for the specified amount of time: Hematoxylin (3-4 minutes), tap water (dip and drain), acid alcohol (2-3 dips or 5-10 seconds), tap water (dip and drain), ammonia water (8-10 dips or 40-50 seconds), tap water (dip and drain), 80% EtOH (2 minutes), Eosin (20-50 seconds).

The samples can be checked under the light microscope for color intensity. If necessary, repeat back to hematoxylin and carry out the sequence once more. This is only possible prior to staining with Eosin reagent, so the samples should be checked prior to this point. Additionally, the time spent in

---

<sup>3</sup> Dr. Matthew Layne in the Biochemistry Department at the Boston University School of Medicine.

Eosin depends on the reagent's freshness. It is easy to over-stain with Eosin, so the samples should be monitored carefully.

Begin to dehydrate the slides by dipping, sequentially, in the following reagents for the specified amount of time: 95% EtOH (dip and drain), 95% EtOH (dip and drain), 100% EtOH (dip and drain), 100% EtOH (2 minutes), xylenes (5 minutes), xylenes (5 minutes).

Following dehydration, mount slides with permount:xylenes or other mounting media and allow the slides to dry in fume hood.

**4.4. Immunohistochemistry Protocol.** Paraffin-embedded sections of mouse tissue are stained using the following immunohistochemistry protocol to visualize specific antigens present in the liver or on blood cells. This allows for the identification and classification of normal or abnormal tissues. As a general rule of thumb, prepare ~40  $\mu$ l of solution for each outlined section to ensure full immersion of tissue section.

To begin, deparaffinize and rehydrate the samples exactly as described in the H&E Staining protocol above (**Method 4.3**). While the samples are being rehydrated, place a beaker of 1.0 L water in microwave for 20 minutes or until boiling for the High Temperature Antigen Retrieval portion of the protocol. It is best to begin heating the water during the deparaffinization and rehydration steps to allow the water to be as hot as possible. After water has begun boiling, pour it into pressure cooker and seal shut to prevent cooling. Fill a Coplin jar or other

appropriately sized container with Na<sup>+</sup>-citrate buffer and microwave until the solution is boiling. It is crucial for High Temperature Antigen Retrieval that this solution is as hot as possible. Save this step until immediately before rehydration is done to ensure the solution does not cool. Place rehydrated samples into Coplin Jar or substitute vessel filled with hot Na<sup>+</sup>-citrate buffer and put Coplin Jar or substitute vessel, covered, in the boiling hot water in the pressure cooker for 30 minutes.

Remove the jar from pressure cooker and allow to cool to room temperature for 20-30 minutes. Drain jar of Na<sup>+</sup>-citrate buffer, disposing of solution in the appropriate waste container and then rinse slides with 1X PBS for 5 minutes.

Remove moisture from slides using Kimwipe, but be sure to not remove the tissue section itself. Outline the tissue section with the Liquid Blocker Super Pap Pen. Draw one circle per antibody and negative control, each one with a diameter of ~1.0 inches. Allow 1 to 2 minutes for pen to dry.

Incubate outlined sections with Cadenza buffer twice, first for 2 minutes and then for 3 minutes. Incubate sections in 3% H<sub>2</sub>O<sub>2</sub> (100 µl 30% H<sub>2</sub>O<sub>2</sub> for every 900 µl of Cadenza buffer) at room temperature for 20 minutes. This step is done in order to block endogenous peroxidase activity and prevent non-specific background staining. Remove H<sub>2</sub>O<sub>2</sub> and wash with Cadenza buffer twice, first for 2 minutes and then for 3 minutes. Block the sections with 5% normal goat serum in Cadenza buffer for 45 minutes at room temperature in a staining box with

damp paper towels. This normal serum is chosen to match the species of the secondary antibody host.

Remove the blocking serum and wash with Cadenza buffer twice, first for 2 minutes and then again for 3 minutes. Incubate the sections with Ki-67 primary antibody overnight at 4°C, diluting in Cadenza buffer at a 1:250 dilution. Remove primary antibody and wash twice with Cadenza buffer, first for 2 minutes and then again for 3 minutes. Incubate sections with diluted secondary antibody in Cadenza buffer for 1 hour at room temperature (1:200 dilution). This secondary antibody should be a Biotinylated Anti-(Primary Antibody Host Species) IgG. About 30 minutes into incubation with the secondary antibody, begin preparing reagents for the Vectastain ABC Kit steps.

Remove the secondary antibody and wash with Cadenza buffer twice, first for 2 minutes and then again for 3 minutes. Incubate the sections with Vectastain ABC Kit (100 µl Cadenza buffer + 1.0 µl reagent A + 1.0 µl reagent B) for 1 hour at room temperature. About 30 minutes into incubation, prepare reagents for the 3,3'-diaminobenzidine (DAB) Substrate Kit step. Remove ABC Kit solution and wash twice with Cadenza buffer, first for 2 minutes and then again for 3 minutes.

Incubate sections with DAB Substrate Kit (2.5 ml Cadenza buffer + 1 drop DAB Buffer (pH = 7.5) + 2 drops DAB substrate + 1 drop H<sub>2</sub>O<sub>2</sub>) in order to produce a brown reaction product in the presence of peroxidase enzyme. This enzyme reaction should be carefully monitored to observe color development and to minimize background from over-incubating. For the Ki-67 primary

antibody, it is suggested to let the reaction incubate for 6-8 minutes, or until noticeably brown. Reaction times vary for each antibody used, so this reaction must be monitored closely if another primary antibody is being used.

Stop enzyme reaction by immersing slides in water for 5 minutes and then counterstain slides in Hematoxylin by dipping, sequentially, in the following reagents for the specified amount of time: Hematoxylin (3-4 minutes), tap water (dip and drain), acid alcohol (2-3 dips or 5-10 seconds), tap water (dip and drain), ammonia water (8-10 dips or 40-50 seconds), tap water (dip and drain). The samples can be checked under the light microscope for color intensity. If necessary, repeat back to hematoxylin and carry out the sequence once more.

Proceed to dehydrate the samples by dipping, sequentially, in the following reagents for the specified amount of time: 80% EtOH (2 minutes), 95% EtOH (dip and drain). Mount slides with Cytoseal or with a Cytoseal:xylenes (1:1) solution and allow to dry in fume hood.

**4.5. Viewing Stained Tissue Under the Light Microscope.** Stained, paraffin-embedded tissue of interest was viewed under the light microscope after being mounted on the positively-charged microscope slides (**Method 4.1**). Both the H&E and immunohistochemistry stains can be examined under the light microscope.

a. *H&E Stained Tissue*

Tissues stained with Hematoxylin and Eosin were viewed under the light microscope at 10X and 40X magnification. Liver sections were examined for infiltration of lymphocytes, observable as strongly basophilic cells that stained with hematoxylin. These cells are approximately 7.5-10  $\mu\text{m}$  in size. Sections of tissue in which an abnormal aggregation of lymphocytes were observed were further examined to determine the number of clusters of lymphocytes viewable within the 10X magnification lens, with clusters being defined as a group of three or more lymphocytes.

Following examination under the light microscope, livers were arbitrarily assigned to one of four classifications: normal, having possible lymphocyte infiltration, having mild lymphocyte infiltration, or as having massive lymphocyte infiltration. Normal livers displayed no obvious signs of lymphocyte infiltration and exhibited a normal morphological phenotype. Livers were classified as having possible lymphocyte infiltration if there appeared to be any sign of abnormal aggregations of basophilic cells, but only if these cells were unable to be confirmed as likely resembling lymphocytes. Livers were classified as having mild lymphocyte infiltration if there was an obvious sign of clusters of lymphocytic cells within the tissue. These clusters were observable in larger numbers than those found in livers classified as having possible lymphocyte infiltration. Livers observed as having massive lymphocyte proliferation had very noticeable infiltration of lymphocytes throughout the tissue, on the scale of greater than 200

(>200) clusters per field. These samples were given to a pathologist who diagnosed the affected mice with leukemia.

b. *Immunohistochemistry with Ki-67 Primary Antibody*

Tissues stained with the immunohistochemistry protocol using the Ki-67 primary antibody were viewed under the light microscope at 10X and 40X magnification. The presence of Ki-67 is identifiable as single cells stained a deep brown color. Liver sections determined to be positive for the presence of Ki-67 were further examined under the 40X magnification lens and arbitrarily assigned to one of three classifications: normal, having mild expression of Ki-67 (+), or having massive expression of Ki-67 (+++). To determine the degree to which each section was Ki-67<sup>+</sup>, the number of Ki-67<sup>+</sup> cells per 40X objective field were counted by hand.

**4.6 Statistical Methods Used in Examination of Stained Tissue Sections.** To ensure an accurate reading of H&E positive cell clusters and Ki-67-positive cells per objective field, multiple readings were taken from the stained tissue sections. Random portions of the liver were chosen for observation under the microscope by simply moving the microscope under the lens and stopping at a random location within the tissue. This was performed a total of three times ( $x_1$ ,  $x_2$ ,  $x_3$ ) for each tissue section. The average number of H&E positive cell clusters or Ki-67-positive cells ( $N_{\text{H\&E}}$  and  $N_{\text{Ki-67}}$ , respectively) was then determined by the following equation:  $N = (x_1 + x_2 + x_3) / 3$ . This method ensures the most accurate reading

of the sample in regards to clusters of lymphocyte infiltration and number of Ki-67<sup>+</sup> cells.

## RESULTS

### *Analysis of liver sections for signs of leukemia and leukocyte infiltration*

Of the twenty-four (24) mice treated in each group (K<sub>i</sub> and WT), twenty-three (23) K<sub>i</sub> and twenty-three (23) WT were available for testing our hypotheses. Mouse liver sample #44 from the K<sub>i</sub> mouse line was found to be unsuccessfully embedded and perfused in paraffin. In addition, one of the WT mice (#11) had not developed a tumor at the end of the study period and was thus not analyzed. None of the mice developed solid tumor metastases from the primary mammary gland tumor. The results of the stains are found in Table 1 and Table 2. Mice numbers labeled in red indicate mice that exhibited poor body conditions.

In the K<sub>i</sub> mouse line, 7 (30.4%) mice showed poor body conditions, compared to 2 (8.7%) WT mice. Two of the K<sub>i</sub> mice with poor body condition suffered from severe dermatitis but for the other 5 mice no obvious cause for their poor health was observed. Four of those 5 K<sub>i</sub> mice (80.0%) suffering from poor body conditions, but not from severe dermatitis, were examined by a pathologist, Dr. Shi Yang<sup>4</sup>, and found to have massive lymphocyte infiltration in the liver consistent with leukemia. The remaining mouse had an enlarged liver and thymus, and while lymphocyte infiltration was visible in the liver it was not elevated to the extent of the other animals.

---

<sup>4</sup> Dr. Shi Yang of the Department of Pathology and Laboratory Medicine at the Boston University School of Medicine.

In contrast, only one liver of the two WT mice with poor body conditions displayed what was classified as massive lymphocyte infiltration. This massive lymphocyte infiltration was consistent with leukemia as determined by Dr. Yang and for the second mouse leukemia/lymphoma diagnosis was also made by Dr. Yang and correlated with strong lymphocyte infiltration in lung tissue (Lim, unpublished)<sup>5</sup>. In conclusion, of the 9 total mice diagnosed with poor body condition, 6 (66.6%; 4 K<sub>i</sub> and 2 WT) were diagnosed with leukemia/lymphoma.

In addition, of the remaining livers examined that did not have leukemia (19 K<sub>i</sub>; 21 WT), 10 K<sub>i</sub> mice out of 19 (52.6%) displayed abnormal lymphocyte infiltration in the liver but to a lesser degree. In comparison, only 5 WT mice out of 21 total (23.8%) displayed abnormal lymphocyte infiltration to a lesser degree in the liver following DMBA treatment. Within the abnormal classifications, 3 K<sub>i</sub> mice (13.0%) had possible lymphocyte infiltration compared to 1 WT mouse (4.3%), 7 K<sub>i</sub> mice (30.4%) had mild lymphocyte infiltration (**Fig. 1B**) compared to 4 WT mice (17.4%). Of the 6 mice classified as having massive lymphocyte infiltration in both WT and K<sub>i</sub> mice, 2 (33.3%) were classified as having portal lymphocyte infiltration (**Fig. 1D**) and 3 (50.0%) were classified as having sinusoidal lymphocyte infiltration (**Fig. 1C**) (Baumhoer, Tzankov, Dirnhofer, Tornillo, & Terracciano, 2008). One WT liver was not available for evaluation. **Figure 2** displays the results of the Hematoxylin and Eosin staining in histogram form.

---

<sup>5</sup> Sarah Lim, undergraduate research assistant in the Kirsch Lab of the Boston University School of Medicine's Biochemistry Department.

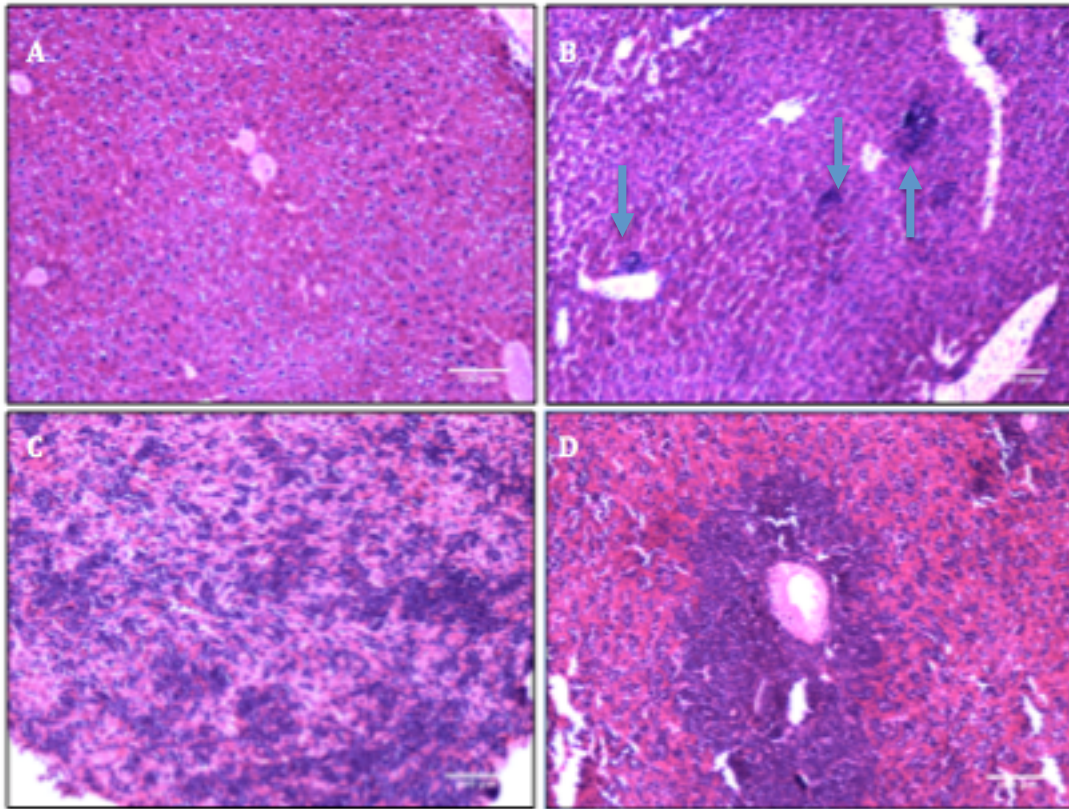


**Figure 1. Livers stained with Hematoxylin and Eosin. a.)** Liver sample from K<sub>i</sub> mouse #969, not treated with DMBA (normal); **b.)** Liver sample from K<sub>i</sub> mouse #17; mild lymphocyte infiltration. The arrows point to “clusters” of lymphocytes; **c.)** Liver sample from K<sub>i</sub> mouse #21; massive sinusoidal lymphocyte infiltration; **d.)** Liver samples from K<sub>i</sub> mouse #56; massive portal lymphocyte infiltration). Scale bar 100μm.

**Table 1.** Results of Hematoxylin and Eosin Staining of K<sub>i</sub> Mouse Livers

| <b>KI</b>     | <b>Available for H&amp;E Analysis: 23</b> |                             |
|---------------|---|-----------------------------|
| Mouse No. (#) | H&E Analysis                              | Avg. H&E Clusters/10x field |
| 2             | Normal                                    |                             |
| 4             | Normal                                    |                             |
| 19            | Normal                                    |                             |
| 23            | Normal                                    |                             |
| 25            | Normal                                    |                             |
| 45            | Normal                                    |                             |
| 46            | Normal                                    |                             |
| 48            | Normal                                    |                             |
| 49            | Normal                                    |                             |
| 7             | Possible lymphocyte infiltration          | 3                           |
| 8             | Possible lymphocyte infiltration          | 1                           |
| 26            | Possible lymphocyte infiltration          | 1.67                        |
| 3             | Mild lymphocyte infiltration              | 0.67                        |
| 5             | Mild lymphocyte infiltration              | 6.33                        |
| 17            | Mild lymphocyte infiltration              | 15.67                       |
| 24            | Mild lymphocyte infiltration              | 2                           |
| 47            | Mild lymphocyte infiltration              | 2.33                        |
| 58            | Mild lymphocyte infiltration              | 1.33                        |
| 65            | Mild lymphocyte infiltration              | 2.67                        |
| 6             | Massive lymphocyte infiltration           | >200                        |
| 15            | Massive lymphocyte infiltration           | >200                        |
| 21            | Massive lymphocyte infiltration           | >200                        |
| 56            | Massive lymphocyte infiltration           | >200                        |
| 44            | Bad sample                                |                             |

**Table 2.** Results of Hematoxylin and Eosin Staining of WT Mouse Livers

| <b>WT</b>     | <b>Available for H&amp;E Analysis: 23</b> |                             |
|---------------|---|-----------------------------|
| Mouse No. (#) | H&E Analysis                              | Avg. H&E Clusters/10x field |
| 10            | Normal                                    |                             |
| 13            | Normal                                    |                             |
| 14            | Normal                                    |                             |
| 29            | Normal                                    |                             |
| 31            | Normal                                    |                             |
| 34            | Normal                                    |                             |
| 35            | Normal                                    |                             |
| 36            | Normal                                    |                             |
| 37            | Normal                                    |                             |
| 38            | Normal                                    |                             |
| 41            | Normal                                    |                             |
| 50            | Normal                                    |                             |
| 51            | Normal                                    |                             |
| 61            | Normal                                    |                             |
| 63            | Normal                                    |                             |
| 64            | Normal                                    |                             |
| 62            | Possible lymphocyte infiltration          | 2.33                        |
| 9             | Mild lymphocyte infiltration              | 4.67                        |
| 32            | Mild lymphocyte infiltration              | 3.33                        |
| 42            | Mild lymphocyte infiltration              | 6.67                        |
| 54            | Mild lymphocyte infiltration              | 5                           |
| 12            | Massive lymphocyte infiltration           | >200                        |
| 59            | Massive lymphocyte infiltration           | >200                        |
| 11            | N/A                                       | N/A                         |

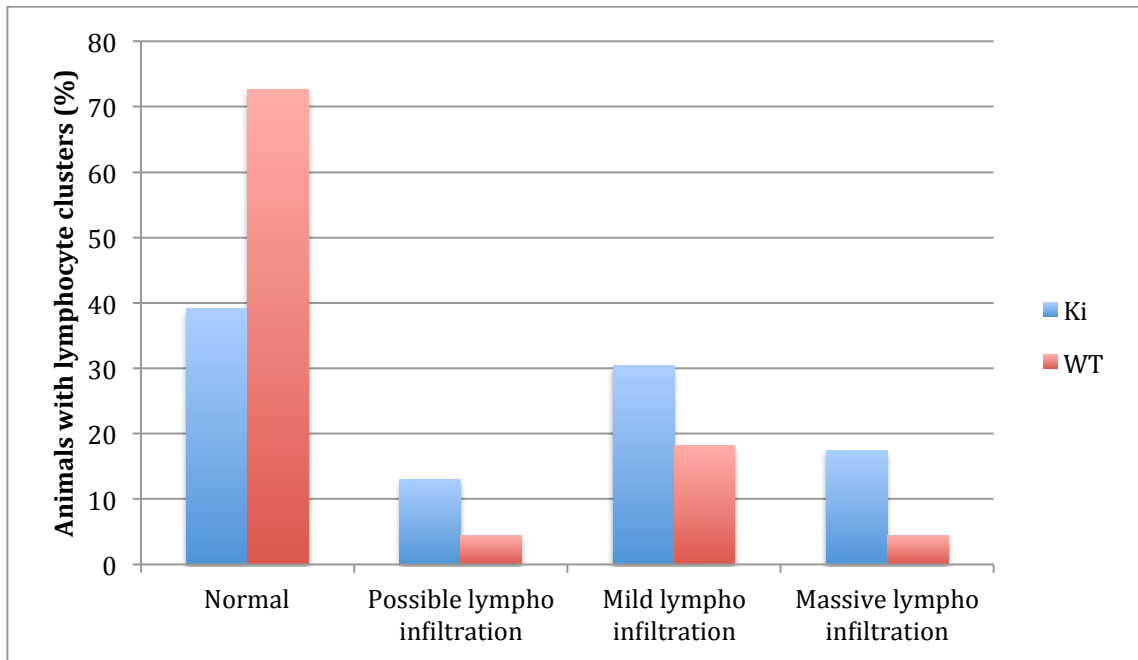


**Figure 2. Lymphocyte infiltration in livers in LOX-PP  $K_i$  vs. WT Mice after treatment with DMBA.** This histogram displays the frequency with which mice were classified as normal or as having possible lymphocyte infiltration, lymphocyte infiltration, or massive lymphocyte infiltration.

### *Cell proliferation measured by Ki-67 Staining*

Twenty-three (23) K<sub>i</sub> and twenty-two (22) WT mouse livers were available for proliferation analysis by immunohistochemistry with Ki-67 antibody. Also included in the Ki-67 analysis were 4 livers from normal mice not treated with DMBA as control samples, two of which are K<sub>i</sub> and two of which are WT. Mouse liver sample #26 from the K<sub>i</sub> mouse line and liver samples #11 and #12 from the WT mouse line were found to be unusable for this experiment. The results of the Ki-67 primary antibody stain are found in Tables 3 and 4.

Of the 23 K<sub>i</sub> mice livers stained with Ki-67, 14 (60.9%) displayed some degree of positivity for the expression of Ki-67, while 10 of the 22 WT mice livers (45.5%) were positive for the expression of Ki-67. Specifically, 3 of the 23 K<sub>i</sub> mice livers (13.0%) were massively positive (+++) (**Fig. 3B,D**) for the expression of Ki-67 while only 1 of the 22 WT mice livers (4.5%) was massively positive for Ki-67. Of the remaining samples, 11 (47.8%) K<sub>i</sub> mice livers slightly positive (+) and 9 (40.9%) WT mice livers were slightly positive (+) for the expression of Ki-67 (**Fig. 3C**). **Figure 4** displays the results of this experiment in histogram form.

In addition, five (5) of the 9 (55.5%) mice stated to have poor body condition tested positive for observable levels of Ki-67 expression. The four livers classified as massively positive for Ki-67 expression (3 K<sub>i</sub> and 1 WT) correlate with mice that had been diagnosed with leukemia/lymphoma. Of the other two mice with leukemia that were not massively positive for Ki-67 expression, 1 was slightly positive for Ki-67 and the other was unavailable for analysis.

**Table 3.** Results of Ki-67 Antibody Immunohistochemistry of K<sub>i</sub> Mice

| KI            | Available for Ki 67 analysis: 23 |                            |
|---------------|----------------------------------|----------------------------|
| Mouse No. (#) | Ki67 Analysis                    | Avg. Ki67+ Cells/40x field |
| 2             | Negative                         |                            |
| 7             | Negative                         |                            |
| 23            | Negative                         |                            |
| 25            | Negative                         |                            |
| 44            | Negative                         |                            |
| 46            | Negative                         |                            |
| 47            | Negative                         |                            |
| 48            | Negative                         |                            |
| 49            | Negative                         |                            |
| 3             | +                                | 59                         |
| 4             | +                                | 56.7                       |
| 5             | +                                | 48                         |
| 8             | +                                | 7.67                       |
| 15            | +                                | 82.7                       |
| 17            | +                                | 85                         |
| 19            | +                                | 36.67                      |
| 24            | +                                | 12.33                      |
| 45            | +                                | 3.3                        |
| 58            | +                                | 7                          |
| 65            | +                                | 49.3                       |
| 6             | +++                              | >200                       |
| 21            | +++                              | >200                       |
| 56            | +++                              | >200                       |
| 024           | +                                | 5                          |
| 969           | +                                | 3                          |
| 26            | N/A                              | Bad sample                 |

**Table 4.** Results of Ki-67 Antibody Immunohistochemistry of WT Mice

| <b>WT</b>     | <b>Available for Ki67 analysis: 22</b> |                            |
|---------------|--|----------------------------|
| Mouse No. (#) | Ki67 Analysis                          | Avg. Ki67+ Cells/40x field |
| 9             | Negative                               |                            |
| 10            | Negative                               |                            |
| 29            | Negative                               |                            |
| 32            | Negative                               |                            |
| 35            | Negative                               |                            |
| 38            | Negative                               |                            |
| 50            | Negative                               |                            |
| 51            | Negative                               |                            |
| 54            | Negative                               |                            |
| 61            | Negative                               |                            |
| 63            | Negative                               |                            |
| 64            | Negative                               |                            |
| 13            | +                                      | 14.3                       |
| 14            | +                                      | 7.7                        |
| 31            | +                                      | 22.3                       |
| 34            | +                                      | 10.3                       |
| 36            | +                                      | 40.7                       |
| 37            | +                                      | 18                         |
| 41            | +                                      | 9.3                        |
| 42            | +                                      | 36                         |
| 62            | +                                      | 40.3                       |
| 59            | +++                                    | >200                       |
| 026           | +                                      | 5                          |
| 684           | +                                      | 8                          |
| 12            | Bad Cut                                | N/A                        |
| 11            | N/A                                    | N/A                        |

### *Correlation Between H&E and Ki-67 Positivity*

Of the 4 K<sub>i</sub> Mice livers classified as having “massive lymphocyte infiltration,” 3 (75.0%) were also classified as being massively positive (++++) for the presence of the Ki-67 antigen. For WT mice, there was a correlation between the massively positive expression of Ki-67 and “massive lymphocyte infiltration” as well, with sample number 59 identifying as massively positive for both lymphocyte infiltration and expression of Ki-67 antigen. In total, 4 (66.7%) of the 6 mouse livers identified as having massive lymphocyte proliferation had a very positive expression of Ki-67 antigen. WT sample #12, a liver with massive lymphocyte infiltration, was unavailable for analysis using immunohistochemistry. It is likely that, if available, it would have also been massively positive for Ki-67 expression.

In total, 18 K<sub>i</sub> mouse livers were classified as positive for either lymphocyte proliferation or for the presence of the Ki-67 antigen. Of these, 11 (61.1%) showed some degree of positivity for both lymphocyte proliferation and for the presence of Ki-67 antigen. For WT mouse livers, a total of 12 livers were classified as positive for either lymphocyte infiltration or for the presence of the Ki-67 antigen. Of these, 3 (25%) showed some degree of positivity for both lymphocyte infiltration and for the presence of Ki-67 antigen.

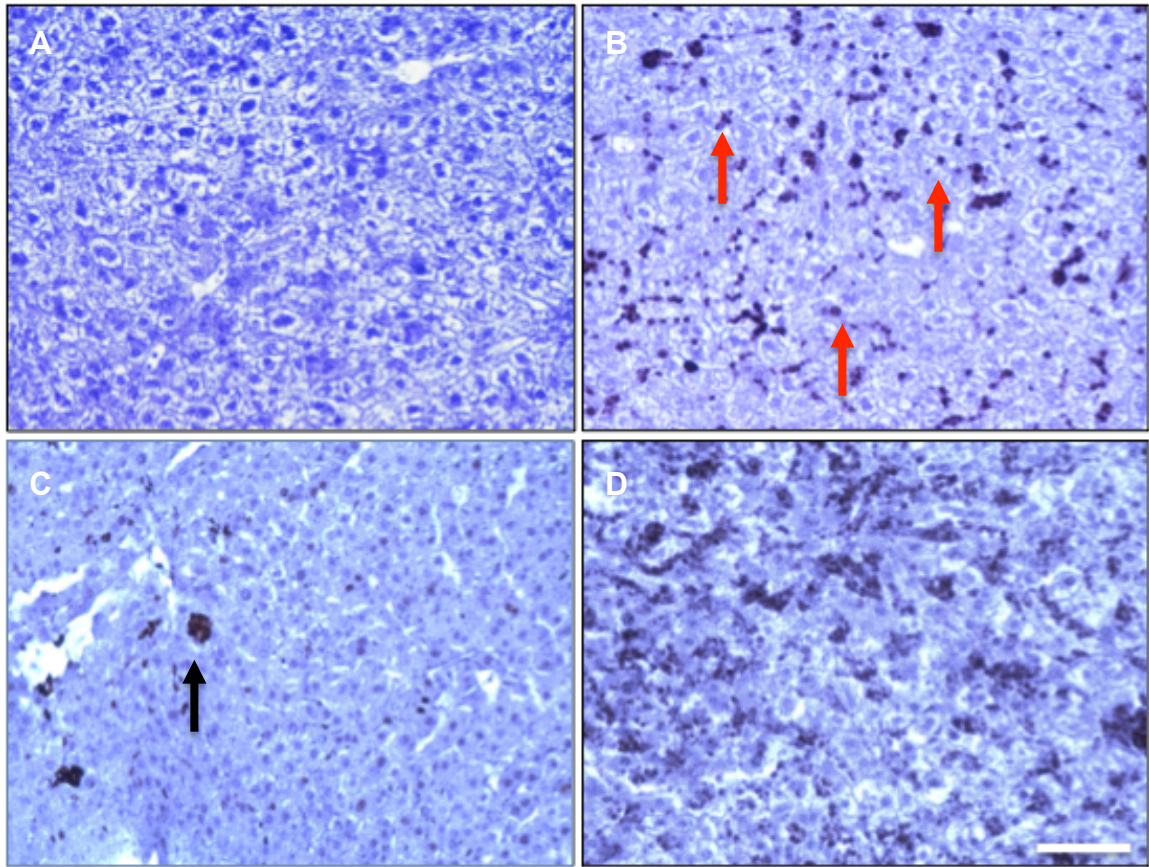


**Figure 3. Livers stained with Ki-67 antibody. a.)** Negative control; **b.)** Liver sample from  $K_i$  mouse sample #59, stained positive for Ki-67 expression; massively positive (+++). **c.)** Liver sample from  $K_i$  mouse sample #19, stained positive for Ki-67 expression; slightly positive (+). **d.)** Liver sample from  $K_i$  mouse sample #21, stained positive for Ki-67 expression; massively positive (+++). Scale bar: 100 $\mu$ m. The red arrows point to individual Ki-67+ cells. The black arrow points to a cluster of Ki-67+ cells.

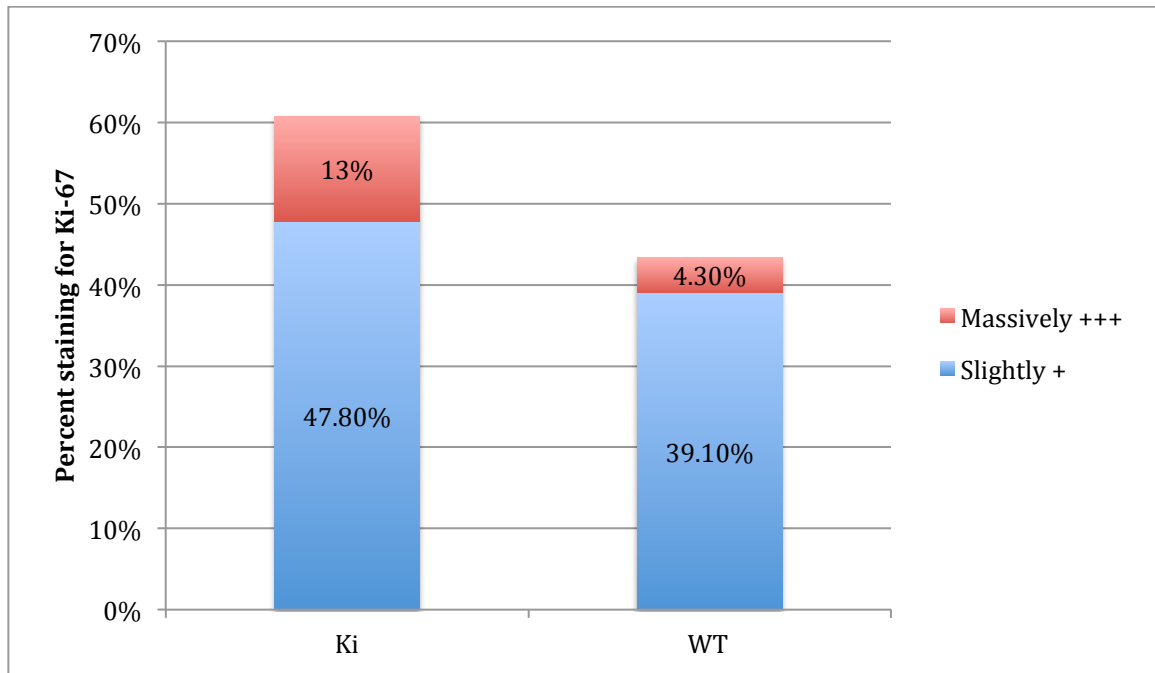


**Figure 4. Expression of Ki-67 in LOX-PP  $K_i$  vs. WT Mice after treatment with DMBA.** This stacked column histogram displays the frequencies with which  $K_i$  and WT mice were classified as being slightly positive (slightly +) or as being massively positive (massively +++) for the expression of Ki-67 following treatment with DMBA.

## DISCUSSION

Knock-in and wild type mice were treated with DMBA and the formation of mammary gland tumors was observed. By the end of the study period, 79.2% of the K<sub>i</sub> mice and 91.6% of the WT mice developed breast cancer. While a greater percentage of WT versus K<sub>i</sub> mice ultimately developed breast cancer, K<sub>i</sub> mice developed tumors more quickly and were more likely to suffer from poor body conditions than their WT counterparts. K<sub>i</sub> mice represented 77.7% of the mice that suffered from poor body conditions (Cueva & Kirsch, unpublished)<sup>6</sup>. These findings corroborate those of Min et al. and others who have previously noted the importance of a functional LOX-PP in the attenuation of invasive and metastatic properties of breast cancer cells and xenograft growth in a mouse model and other cancers.

Interestingly, a number of DMBA-treated mice suffering from poor body conditions showed no signs of having developed breast cancer. We hypothesized that these mice suffered from leukemia or some other lymphoproliferative disease and, in following with the work of Huggins et al., we focused our search for these diseases on the liver. Indeed, our analyses of H&E stained mouse livers showed abnormal lymphocyte infiltration characteristic of leukemia or other lymphoproliferative diseases in 60.9% of LOX-PP K<sub>i</sub> mice and in 29.2% of WT mice livers. Following analysis by a pathologist, six of the mice (4

---

<sup>6</sup> Unpublished study conducted by Dr. Ana de la Cueva and Dr. Kathrin H. Kirsch in the Biochemistry Department at the Boston University School of Medicine.

K<sub>i</sub> and 2 WT) displaying abnormal lymphocyte infiltration were diagnosed with leukemia or lymphoma. These diagnoses correlated to those mice who suffered from poor body conditions but that were not diagnosed with breast cancer. That these mice were diagnosed with leukemia supports our hypotheses that unexplained poor body conditions would be due to leukemia or other lymphoproliferative diseases. Additionally, that 66.7% of all diagnosed leukemias were found in K<sub>i</sub> mice harboring the LOX-PP<sub>v</sub> supports our hypothesis that, if present, leukemia or some other lymphoproliferative disease would be more present in K<sub>i</sub> than in WT mice.

Furthermore, our experiment demonstrated that K<sub>i</sub> mice were more likely to express the nuclear proliferation-associated protein Ki-67 than WT mice when exposed to DMBA (60.8% versus 41.7%, respectively). It was also noted that the expression levels of Ki-67 reached observable levels in 5 of the 9 (55.5%) mice with poor body conditions, which supports previous findings that Ki-67 is a cellular proliferation marker indicative of a negative patient prognosis (Niikura et al., 2014; Scholzen & Gerdes, 2000).

In both K<sub>i</sub> and WT mice, there did appear to be a similarity in the physical distribution of both the basophilic lymphocytes in H&E and Ki-67<sup>+</sup> cells within the tissue, suggesting that the lymphocytes themselves could be expressing the nuclear proliferative signal. This observation is noticeable when comparing H&E staining and Ki-67 immunohistochemistry from K<sub>i</sub> mouse sample #21 (**Fig. 1C**, **Fig. 3D**). Both figures display cells as evenly distributed throughout the hepatic

sinusoids. Additionally, preliminary comparisons of H&E staining and Ki-67 immunohistochemistry from DMBA-treated mice have demonstrated similar findings, especially amongst livers in mice definitively diagnosed with leukemia.

Despite these findings, however, our research does not appear to show an absolute correlation between the degree of positivity for lymphocyte infiltration in H&E and Ki-67 expression levels, as 12 total mice expressed observable levels of Ki-67 but had little or no visible lymphocyte cluster infiltration abnormalities found in H&E analyses. Additionally, in mice that do show positive readings for both H&E and expression of Ki-67, there does not appear to be a correlation between number of H&E clusters and number of Ki-67<sup>+</sup> cells. This could be due, however, to the fact that Ki-67<sup>+</sup> readings indicate mostly single cells as expressing the antigen. In contrast, a positive H&E reading for abnormal lymphocyte infiltration was scored by the presence of aggregates of 3 or more basophilic cells to test positive. These clusters were rarely or not seen to be positive for Ki-67. Thus, it is possible that abnormal lymphocyte infiltration was present and simply not scored in livers that tested positive for Ki-67 expression.

Given the nature of H&E staining and the antibody used in our immunohistochemistry analysis, we are unable to say definitively that the abnormal lymphocyte infiltration present in the livers of mice not diagnosed by the pathologist as having leukemia are, indeed, indicative of early manifestations of leukemia or other lymphoproliferative diseases. Future research could be directed to the identification and classification of these basophilic and Ki-67<sup>+</sup> cells

in order to more accurately diagnose the cause of these abnormalities discovered in the liver. This could be done by staining for an antigen specific to leukemic cells or by conducting blood tests. Unfortunately, blood was not extracted and preserved from these mice prior to their sacrifice and disposal. As Huggins and Sugiyama demonstrated, it is helpful in the analysis and diagnosis of leukemia to procure blood from the periphery for analysis of leukocyte count, hematocrit, hemoglobin, and smeared blood films. Coupled with a liver biopsy, this is the best way to detect leukemia (Huggins & Sugiyama, 1966).

Our research has thus further established the importance of LOX-PP in the attenuation and propagation of cancer. In its absence, mice are noticeably more likely to develop and succumb to poor body conditions, show noticeable lymphocyte infiltration in the liver indicative of leukemia and other lymphoproliferative diseases, and display the cellular proliferation marker Ki-67. Our findings therefore suggest that LOX-PP is not only important in the attenuation of breast cancer, but that a malfunctioning LOX-PP could result in a greater likelihood of leukemia or some other lymphoproliferative disease.

## REFERENCES

- American Cancer Society. Cancer Facts & Figures 2016. Atlanta: American Cancer Society; 2016
- Barker, H. E., Cox, T. R., & Erler, J. T. (2012). The rationale for targeting the LOX family in cancer. *Nature Reviews Cancer*, 12(8), 540–552. <http://doi.org/10.1038/nrc3319>
- Baumhoer, D., Tzankov, A., Dirnhofer, S., Tornillo, L., & Terracciano, L. M. (2008). Patterns of liver infiltration in lymphoproliferative disease. *Histopathology*, 53(1), 81–90. <http://doi.org/10.1111/j.1365-2559.2008.03069.x>
- Chan, K. K., Matchett, K. B., McEnhill, P. M., Dakir, E. H., McMullin, M. F., El-Tanani, Y., ... El-Tanani, M. (2015). Protein deregulation associated with breast cancer metastasis. *Cytokine and Growth Factor Reviews*, 26(4), 415–423. <http://doi.org/10.1016/j.cytogfr.2015.05.002>
- Contente, S., Kenyon, K., Rimoldi, D., & Friedman, R. M. (1990). Expression of gene rrg is associated with reversion of NIH 3T3 transformed by LTR-c-H-ras. *Science*, 249(4970), 796–798. <http://doi.org/10.1126/science.1697103>
- Csiszar, K. (2001). Lysyl oxidases: a novel multifunctional amine oxidase family. *Progress in Nucleic Acid Research and Molecular Biology*, 70, 1–32.
- Csiszar, K., Mariani, T. J., Gosin, J. S., Deak, S. B., & Boyd, C. D. (1993). A restriction fragment length polymorphism results in a nonconservative amino acid substitution encoded within the first exon of the human lysyl

oxidase gene. *Genomics*, 16(2), 401–406.

<http://doi.org/10.1006/geno.1993.1203>

Currier, N., Solomon, S. E., Demicco, E. G., Chang, D. L. F., Farago, M., Ying, H., ... Seldin, D. C. (2005). Oncogenic Signaling Pathways Activated in DMBA-Induced Mouse Mammary Tumors. *Toxicologic Pathology*, 33(6), 726–737. <http://doi.org/10.1080/01926230500352226>

Giampuzzi, M., Botti, G., Cilli, M., Gusmano, R., Borel, A., Sommer, P., & Donato, A. D. (2001). Down-regulation of Lysyl Oxidase-induced Tumorigenic Transformation in NRK-49F Cells Characterized by Constitutive Activation of Ras Proto-oncogene. *Journal of Biological Chemistry*, 276(31), 29226–29232. <http://doi.org/10.1074/jbc.M101695200>

Hanahan, D., & Weinberg, R. A. (2011). Hallmarks of Cancer: The Next Generation. *Cell*, 144(5), 646–674.

<http://doi.org/10.1016/j.cell.2011.02.013>

Huggins, C. B., & Sugiyama, T. (1966). Induction of leukemia in rat by pulse doses of 7,12-dimethylbenz(a)anthracene. *Proceedings of the National Academy of Sciences of the United States of America*, 55(1), 74–81.

Hwang, J. J., Lee, D. H., Lee, A.-R., Yoon, H., Shin, C. M., Park, Y. S., & Kim, N. (2015). Characteristics of gastric cancer in peptic ulcer patients with *Helicobacter pylori* infection. *World Journal of Gastroenterology : WJG*, 21(16), 4954–4960. <http://doi.org/10.3748/wjg.v21.i16.4954>

Jeay, S., Pianetti, S., Kagan, H. M., & Sonenshein, G. E. (2003). Lysyl Oxidase

Inhibits Ras-Mediated Transformation by Preventing Activation of NF- $\kappa$ B.

*Molecular and Cellular Biology*, 23(7), 2251–2263.

<http://doi.org/10.1128/MCB.23.7.2251-2263.2003>

Jong, M. de, & Maina, T. (2010). Of Mice and Humans: Are They the Same?—

Implications in Cancer Translational Research. *Journal of Nuclear*

*Medicine*, 51(4), 501–504. <http://doi.org/10.2967/jnumed.109.065706>

Liu, J.-L., Wei, W., Tang, W., Jiang, Y., Yang, H.-W., Li, J.-T., & Zhou, X. (2012).

Silencing of lysyl oxidase gene expression by RNA interference

suppresses metastasis of breast cancer. *Asian Pacific Journal of Cancer*

*Prevention: APJCP*, 13(7), 3507–3511.

Lorusso, G., & Rüegg, C. (2012). New insights into the mechanisms of organ-

specific breast cancer metastasis. *Seminars in Cancer Biology*, 22(3),

226–233. <http://doi.org/10.1016/j.semcancer.2012.03.007>

McCuskey, R. (2012). Chapter 1 - Anatomy of the Liver A2 - Sanyal, Thomas D.

BoyerMichael P. MannsArun J. In *Zakim and Boyer's Hepatology (Sixth*

*Edition)* (pp. 3–19). Saint Louis: W.B. Saunders. Retrieved from

<http://www.sciencedirect.com/science/article/pii/B9781437708813000012>

Min, C., Kirsch, K. H., Zhao, Y., Jeay, S., Palamakumbura, A. H., Trackman, P.

C., & Sonenshein, G. E. (2007). The tumor suppressor activity of the lysyl

oxidase propeptide reverses the invasive phenotype of Her-2/neu-driven

breast cancer. *Cancer Research*, 67(3), 1105–1112.

<http://doi.org/10.1158/0008-5472.CAN-06-3867>

- Min, C., Yu, Z., Kirsch, K. H., Zhao, Y., Vora, S. R., Trackman, P. C., ...  
Sonenshein, G. E. (2009). A loss-of-function polymorphism in the propeptide domain of the LOX gene and breast cancer. *Cancer Research*, 69(16), 6685–6693. <http://doi.org/10.1158/0008-5472.CAN-08-4818>
- Min, C., Zhao, Y., Romagnoli, M., Trackman, P. C., Sonenshein, G. E., & Kirsch, K. H. (2010). Lysyl Oxidase Propeptide Sensitizes Pancreatic and Breast Cancer Cells to Doxorubicin-Induced Apoptosis. *Journal of Cellular Biochemistry*, 111(5), 1160–1168. <http://doi.org/10.1002/jcb.22828>
- Niikura, N., Masuda, S., Kumaki, N., Xiaoyan, T., Terada, M., Terao, M., ...  
Tokuda, Y. (2014). Prognostic Significance of the Ki67 Scoring Categories in Breast Cancer Subgroups. *Clinical Breast Cancer*, 14(5), 323–329.e3. <http://doi.org/10.1016/j.clbc.2013.12.013>
- Nishioka, T., Eustace, A., & West, C. (2012). Lysyl Oxidase: From Basic Science to Future Cancer Treatment. *Cell Structure and Function*, 37(1), 75–80. <http://doi.org/10.1247/csf.11015>
- Oeffinger KC, Fontham aEH, Etzioni R, et al. Breast Cancer Screening for Women at Average Risk: 2015 Guideline Update From the American Cancer Society. *JAMA*.2015;314(15):1599-1614.  
doi:10.1001/jama.2015.12783.
- Palamakumbura, A. H., Jeay, S., Guo, Y., Pischon, N., Sommer, P., Sonenshein, G. E., & Trackman, P. C. (2004). The Propeptide Domain of Lysyl Oxidase Induces Phenotypic Reversion of Ras-transformed Cells. *Journal of*

*Biological Chemistry*, 279(39), 40593–40600.

<http://doi.org/10.1074/jbc.M406639200>

Protocol for the Preparation of Gelatin-coated Slides for Histological Tissue Sections. (n.d.). Retrieved March 13, 2016, from <https://www.rndsystems.com/resources/protocols/protocol-preparation-gelatin-coated-slides-histological-tissue-sections>

Romero, R. M. (2005). *Trends in Leukemia Research*. Nova Publishers.

Scholzen, T., & Gerdes, J. (2000). The Ki-67 protein: from the known and the unknown. *Journal of Cellular Physiology*, 182(3), 311–322.

[http://doi.org/10.1002/\(SICI\)1097-4652\(200003\)182:3<311::AID-JCP1>3.0.CO;2-9](http://doi.org/10.1002/(SICI)1097-4652(200003)182:3<311::AID-JCP1>3.0.CO;2-9)

Tabariès, S., Annis, M. G., Hsu, B. E., Tam, C. E., Savage, P., Park, M., & Siegel, P. M. (2015). Lyn modulates Claudin-2 expression and is a therapeutic target for breast cancer liver metastasis. *Oncotarget*, 6(11), 9476–9487.

Zhang, C., Xu, Y., Hao, Q., Wang, S., Li, H., Li, J., Gao, Y., Li, M., Li, W., Xue, X., Wu, S., Zhang, Y. and Zhang, W. (2015), FOXP3 suppresses breast cancer metastasis through downregulation of CD44. *Int. J. Cancer*, 137: 1279–1290. doi: 10.1002/ijc.29482

## CURRICULUM VITAE

### **MICHAEL EMMERLING**

Address: 16 Stone St., Macedon, NY 14502 • Phone: (585) 545-8437

E-mail: memmerli@bu.edu • Birth Year: 1992

### **EDUCATION**

**Boston University School of Medicine**, Boston, MA 09/14 – Present  
M.S. in Medical Sciences [expected 05/16]

**Boston College**, Chestnut Hill, MA 09/10 – 05/14  
B.S. in Biology

### **RESEARCH**

**Boston University School of Medicine**, Boston, MA 06/15 – Present  
*Graduate Research Assistant*

- Conducted histological analyses on mice livers to observe the role of a variant lysyl oxidase propeptide (LOX-PP<sub>v</sub>) in DMBA-induced cancer development in mice

**Flaum Eye Institute**, University of Rochester, Rochester, NY 06/13 – 09/13  
*Lab Assistant*

- Conducted research on the dynamics of tear film breakup in patients diagnosed with dry-eye syndrome, specifically those afflicted with aqueous deficient dry eye or meibomian gland dysfunction
- Learned proper laboratory protocols for clinical-trials and became familiarized with complex laboratory techniques like optical coherence tomography and thermal imaging

**Investigations in Molecular Cell Biology**, Chestnut Hill, MA 06/11 – 12/11  
*Student*

- Collected and analyzed series of data to study gene knockouts in mutated strains of *Saccharomyces cerevisiae*
- Utilized a variety of laboratory techniques like PCR, gel electrophoresis, SDS-PAGE, and Western blots to restore strains to a functional phenotype

### **VOLUNTEER EXPERIENCE**

**Boston Medical Center bWell Center**, Boston, MA 01/15 - 12/15  
*Volunteer*

- Engaged in a variety of health and fitness activities with pediatrics patients for three hours every week

- Acted as a resource for pediatrics patients and their families to empower them with information necessary to make healthy lifestyle choices

**Peer Health Exchange**, Chestnut Hill, MA 10/12 – 05/13  
*Health Educator*

- Constructed fun, informative lesson plans on how to lead a healthy lifestyle and thereafter presented them to ninth graders in urban Boston schools
- Collaborated with peers in weekly workshops to improve communication and teaching skills
- Specialized in drug and alcohol education

**PROFESSIONAL EXPERIENCE**

**Boston College Interactive Media**, Chestnut Hill, MA 01/11 – 05/14  
*Media Crew*

- Filmed and worked sporting events for Boston College’s Division I collegiate teams
- Operated film cameras, scoreboard, and replay machine during events, and thereafter assisted in the production of post-game videos

**ADT Security Systems**, Rochester, NY 05/12 – 08/12  
*Outbound Representative*

- Dealt directly with ADT customers and assisted in the scheduling of appointments for security system maintenance

**CLUBS/ORGANIZATIONS**

**Boston University MAMS Subcommittee**, Boston, MA 03/15 - Present  
*Committee Member/Social Media Representative*

- Acted as liaison between current MAMS students and faculty
- Interacted with prospective MAMS students at open houses, on campus tours, and via email or other social media venues such as Student Doctor Network and FaceBook
- Held monthly meetings with the director of the MAMS program to discuss upcoming program events and to bring student inquiries to the attention of the faculty